Excitation Requirement For Rectified Output AC Generators

Richard Thomas Smith
Missouri University of Science and Technology

In the concept of striking distance to be used even in the future, the author believes that $\bar{r}_s$ varies with increasing r and I. That means that for a certain value of I, $\bar{r}_s$ cannot be drawn as a part of a circle around the shielding wire; for example, the curve is more flat on the top and it decreases fast for higher values of r.

The calculations of an actual transmission line should, as Prof. Whitehead mentioned, be completed for the midspan clearances. This can be done by using the "new" values of the shielding and phase wires' heights over the ground at midspan. The calculations are in principle the same as those presented in the paper. By studying the critical shielding angles for each phase wire at the tower and along the line, one can predict the maximum values that give effective shielding.

Dr. Fisher points out that the critical value of 10 kV/cm for strokes to the ground may be somewhat high and that the value of 7.5 kV/cm might be better. This may be true in some cases, but the author feels that more experimental data are needed before a more accurate value can be stated. However, the calculations of the 130-kV transmission line described in the paper were repeated for various critical values including 7.5 kV/cm. Moreover, the Ohio Valley Electric Company (OVEC) 345-kV system was studied with both critical values of 10 kV/cm and 7.5 kV/cm. The results of these studies show that the change of the critical field strength from 10 kV/cm to 7.5 kV/cm causes small variations in the covered area (compare Table VI to Table III and Table VII to Table VIII), but indicates the same probable shielding failures.

The covered (or shielded) area changes with stroke amplitudes as may be observed from the various tables. It increases with increasing values of stroke amplitudes or charge densities. As for other assumptions of charge density, some calculations were made, the results of which proved that the shielded area did not change radically with different assumptions. Even in an extreme case picturing a charge with a uniform charge density, a charge "tip" whose length is 50 meters, and a charge density twice the density of the "tail," α for the transmission system described in the paper increases from 4.5 to 5.8 strokes per 100 km per year only. The propagation velocity of the charges v is low compared with the propagation of the electromagnetic field, thus even big changes in v cause negligible changes of the shielded area.

Calculations of the OVEC 345-kV system show that probable strokes to phase wire 2 (middle phase wire) are to be expected for stroke amplitudes up to about 10 kA (see Table VII). This may explain shielding failures for phase wire 2 reported in several observed data. For this tower configuration the various shielding angles are: for phase wire 1 (top) about 35°, for phase wire 2 (middle) about 26°, and for phase wire 3 (bottom) about 15°. That means that in this case the angle of 26° for phase wire 2 is not enough if shielding failures are to be avoided.

Fig. 10 is calculated from a curve presented in [19]. This curve is based on data from several different sources and predicts higher values of stroke amplitudes than those given in the old AIEE curve. However, some changes of $p(I)$ have a small influence on the calculated values of α.

As Dr. Fisher points out, the procedure described in the paper can be applied for predicting the protection of structures. As it can be observed from Table I the radius for which strokes are still attracted to a tall object varies with stroke amplitudes. It varies for an object 30 meters high from 10 meters ($I = 5$ kA) to 40 meters ($I = 100$ kA); whereas for an object 46 meters high, it varies from 10 meters ($I = 5$ kA) to 45 meters ($I = 100$ kA). This means that caution should be used in dealing with the concept of the 45° cone of protection. It may hold for certain heights through a wide spectrum of stroke amplitudes, but for other objects this may be true only for a narrower band of amplitudes.

Excitation Requirement for Rectified Output AC Generators

RICHARD T. SMITH

Abstract—**This paper develops a method for calculating the required dc field current of a three-phase synchronous ac generator for known dc load conditions and machine characteristics. The method is simple to apply and has shown good agreement with test data. The method is of utility for preliminary design and analysis of rectified output alternators, such as may be used in excitation systems of the largest ac generators, space vehicle power applications, or high-power industrial rectification.**

Paper 70 TP 14-PWR, recommended and approved by the Rotating Machinery Committee of the IEEE Power Group for presentation at the IEEE Winter Power Meeting, New York, N. Y., January 25–30, 1970. Manuscript submitted August 19, 1969; made available for printing October 22, 1969.

The author was with the Electric Power Engineering Curriculum, Rensselaer Polytechnic Institute, Troy, N. Y. He is now with the Department of Electrical Engineering, University of Missouri, Rollo, Mo. 65401.

Introduction

In recent years several new applications for rectified output rotating ac generators have been developed. These include excitation systems for very large turbogenerators as well as power plants for future space vehicles. One of the important aspects of these generator-rectifier systems is the steady-state relationship between dc field current and rectified load (dc) output voltage and current. A study of [1]–[6] shows little reported specifically in this area, except for the work of Shilling.

This paper develops a simple method based upon an approximate representation of the system and tests its efficacy by comparing calculated and experimental data. The method is applied to two different conditions of operation: constant load voltage, such as might be obtained with a large capacitor across the load resistance, and constant load current, insured by a large

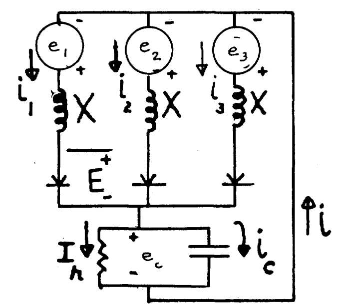

(a)

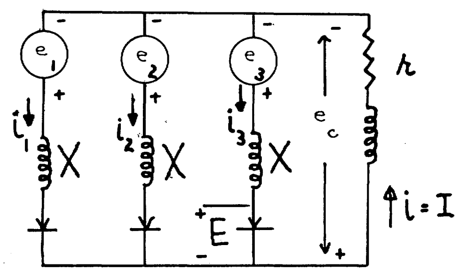

(b)

Fig. 1. Representations and connections of generator-rectifier system studied. (a) Constant load voltage. (b) Constant load current.

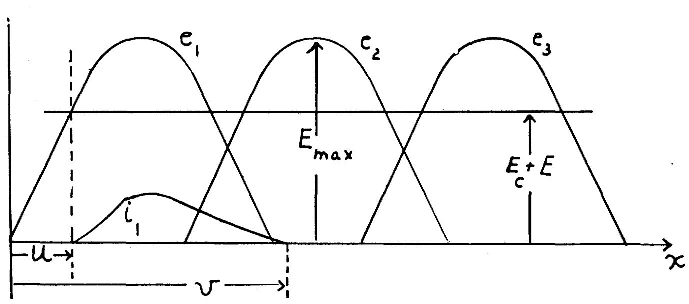

(a)

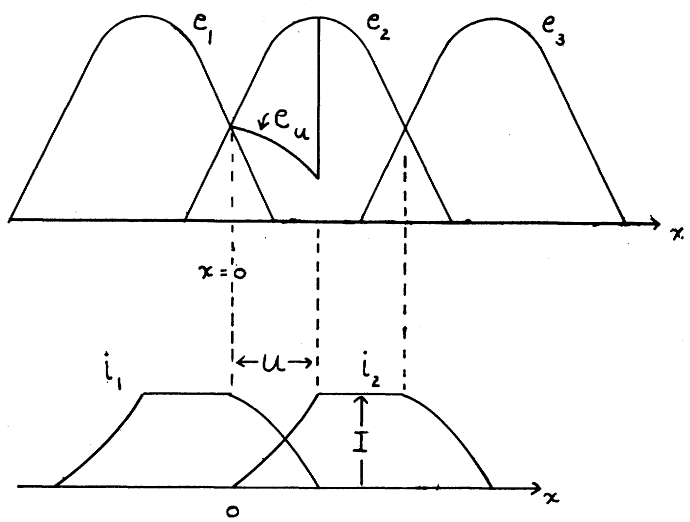

(b)

Fig. 2. Voltage and current relationships. (a) Constant load voltage. (b) Constant load current.

inductor in series with the load resistance. The analysis considers only a three-phase star-connected generator-rectifier system (Fig. 1) but can be extended to other connections. Only the time fundamentals of the generator current and voltage are utilized in determining the excitation requirement, and generator resistance is assumed negligible.

Analysis

Constant Load Voltage

In Fig. 2(a) e_1 represents the instantaneous sinusoidal value of phase-1 "air gap" voltage, behind the effective reactance X at normal angular frequency ω. E is the rectifier forward constant voltage drop. i_1 is the instantaneous current in phase 1 of the generator. The load voltage, because of the condenser, remains constant at $e_c = E_c$. Resistance effects will be neglected.

During conduction by anode 1

$$e_1 - X \frac{di_1}{dx} = E + E_c \tag{1}$$

where

$$x = \omega t$$
$$e_1 = E_{max} \sin x.$$

In accordance with Fig. 2(a) we assume conduction begins at $x = u$, and ceases at $x = v$. Then

$$\sin u = \frac{E_c + E}{E_{max}} \tag{2}$$

and

$$(u - v) \sin u + \cos u - \cos v = 0. \tag{3}$$

Equation (3) is a consequence of i_1 equaling zero at $x = u$ and $x = v$, the expression for i_1 from (1) being

$$\frac{Xi_1}{E} = \frac{E + E_c}{E_{max}} (u - x) - \cos x + \cos u.$$

The dc component I_r of the rectified current flows only through the load resistance, and the harmonic time-varying components i_c flow mainly through the large capacitor. But

$$I_r = \frac{1}{2\pi} \int_{x_1}^{x_1 + 2\pi} (i_1 + i_2 + i_3) dx. \tag{4}$$

i_2 and i_3 have the same shape as i_1. Thus we find

$$I_r = \frac{3E_{max}}{2\pi X} \left[\frac{(v - u)}{2} (\cos u + \cos v) + \sin u - \sin v \right]. \tag{5}$$

By combining (2), (3), and (5) we can write

$$\frac{2\pi X I_r}{3(E_c + E)} = g(u). \tag{6}$$

The function $g(u)$ is plotted in Fig. 3. If X, I_r, E_c, and E are known for a particular operating condition, then the left side of (6) may be quickly calculated and the value of u found from Fig. 3. When u has been determined (2) can be used to calculate E_{max}. Knowing E_{max}, if we can find the fundamental frequency component of the phase-1 current we can complete a phasor diagram (Fig. 4) to establish the required excitation. The fundamental frequency component of phase current is established

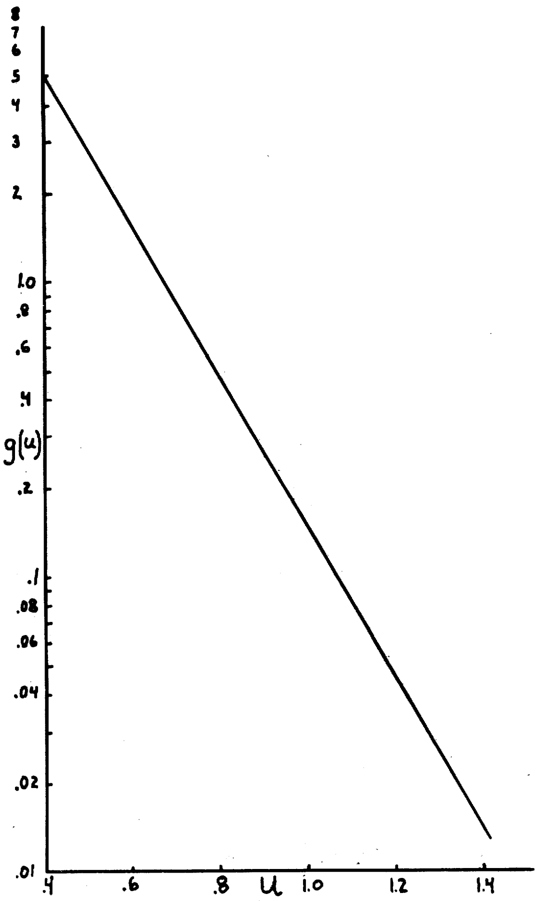

Fig. 3. Function $g(u)$ versus u.

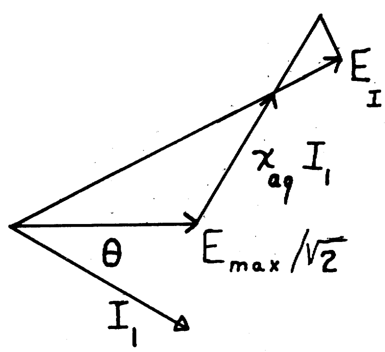

Fig. 4. Phasor diagram for synchronous machine.

as follows: we assume the current

$$i_1 = \Sigma(A_n \sin nx + B_n \cos nx) \tag{7}$$

from which we find

$$A_1 \frac{\pi X}{E_{\max}} = \frac{(\sin v - \sin u)^2}{2} \tag{8}$$

$$B_1 \frac{\pi X}{E} = -\frac{(v-u)}{2} - \sin u \cos v + \frac{\sin 2u + \sin 2v}{4}. \tag{9}$$

A plot of

$$H = \frac{\pi X}{E_{\max}} (A_1{}^2 + B_1{}^2)^{1/2} \tag{10}$$

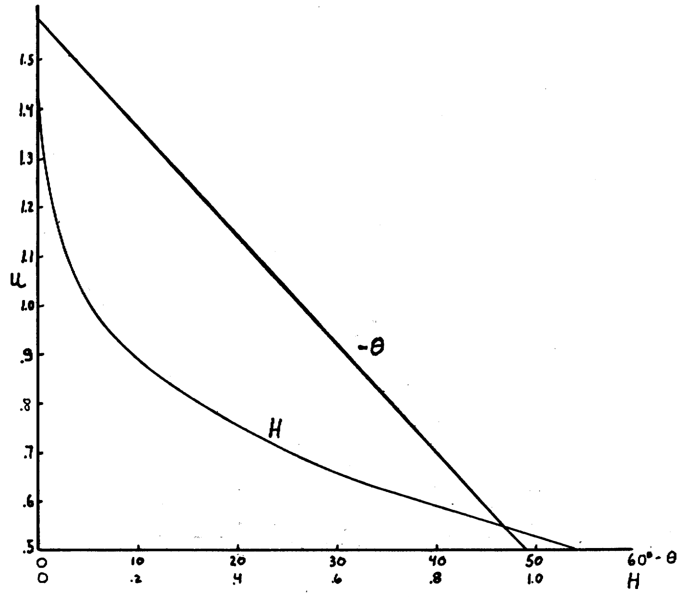

Fig. 5. H and $-\theta$ as functions of u.

and

$$-\theta = \tan^{-1} - \frac{B_1}{A_1} \tag{11}$$

versus u—v is eliminated by using (3)—is shown in Fig. 5. Since u is known, we can use Fig. 5 to find H and $-\theta$, where $-\theta$ is the angle by which the fundamental component of i_1 lags e_1. The rms magnitude of the fundamental component of i_1 is denoted by I_1:

$$I_1 = \frac{HE_{\max}}{\pi X\sqrt{2}}. \tag{12}$$

After completing the phasor diagram of Fig. 4, using $x_{aq} = x_q - X$ and $x_{ad} = x_d - X$, the field current can be read directly from an open-circuit curve. A more refined method for including saturation may also be used if desirable.

Constant Load Current

For constant load current conditions we assume that there is a large choke in series with the load resistance, as shown in Fig. 1(b).

We will let $e_1 = E_{\max} \cos (x + \pi/3)$, and assume that there will be a conduction pattern like that shown in Fig. 2(b). Now

$$i_1 = I - \frac{E_{\max}}{X} (1 - \cos x) \sin \frac{\pi}{3} \tag{13}$$

$$i_2 = \frac{E_{\max}}{X} (1 - \cos x) \sin \frac{\pi}{3}. \tag{14}$$

Because i_1 is zero when $x = u$, we find from (13)

$$\cos u = 1 - \frac{IX}{E_{\max} \sin \pi/3}. \tag{15}$$

The load dc voltage is found to be

$$E_d = \frac{3E_{\max}\sqrt{3}}{4\pi} (1 + \cos u). \tag{16}$$

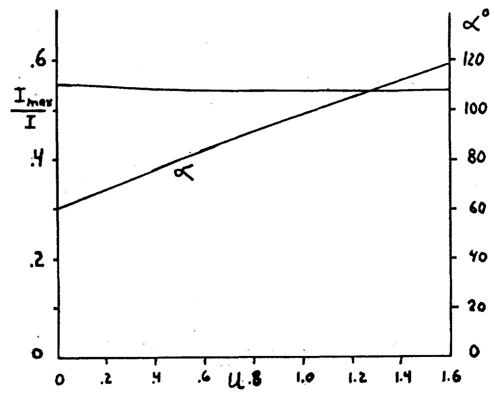

Fig. 6. $I_{\max}/I$ and α as functions of u.

In order to account for the rectifier drop E, we will add it to E_d, giving

$$E_d + E = \frac{3E_{\max}\sqrt{3}}{4\pi}(1 + \cos u). \tag{17}$$

We note that the above relations hold true for $u \le \pi/2$.

Next we determine the relation between the dc load current I and the fundamental frequency component of current flowing in phase 2. Let

$$i_2 = A_0 + \Sigma(A_n \cos nx + B_n \sin nx). \tag{18}$$

After tedious integration we find

$$\frac{A_1\pi}{I\sqrt{3}} = -\sin(u - \pi/6) + \frac{1}{1 - \cos u} \cdot \left[\sin(u - \pi/6) - \frac{1}{4}\sin(2u - \pi/6)\right] \tag{19}$$

and

$$\frac{B_1\pi}{I\sqrt{3}} = \cos(u - \pi/6) + \frac{1}{1 - \cos u} \cdot \left[-\cos(u - \pi/6) + \frac{11}{8} + \frac{u}{4} - \frac{\sin^2 u}{2\sqrt{3}} - \frac{1}{4\sqrt{3}}\cos(2u + 2\pi/3)\right]. \tag{20}$$

We can write

$$i_{2_{\text{fund}}} = (A_1^2 + B_1^2)^{1/2}\cos(x - \alpha) = I_{\max}\cos(x - \alpha) \tag{21}$$

where $\alpha = \tan^{-1} B_1/A_1$.

The angle by which e_2 leads $i_{2_{\text{fund}}}$ is $\alpha - \pi/3$. Fig. 6 shows curves of $I_{\max}/I$ and α versus u.

We now have all the basic data needed to calculate the excitation requirement for the constant load current condition. By combining (15) and (17) we have

$$E_{\max} = \frac{2\pi}{3\sqrt{3}}(E_d + E) + \frac{IX}{\sqrt{3}}. \tag{22}$$

For known load conditions and X we can use (22) to calculate $E_{\max}$. We next use (15) to find u. Fig. 6 gives us $I_{\max}/I$ and α for the corresponding u, and thus we can draw the phasor diagram (like Fig. 4) to find the excitation.

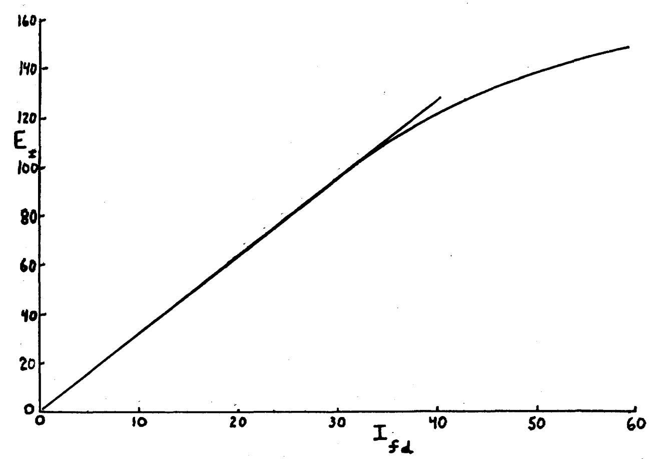

Fig. 7. No-load saturation curve for test machine.

TABLE I

TEST DATA FOR CONSTANT VOLTAGE

Load Voltage, E_c (volts)	Load Current, I_1 (amperes)	Field Current Measured (amperes)	Field Current Calculated (amperes)
80	40	29.5	28
60	100	33.3	37
100	100	50.5	56

TESTS AND CALCULATIONS

Tests were carried out on a 400-Hz aircraft-type three-phase 3000-r/min generator, rated at 30 kVA, 120 volts line to neutral. Pertinent calculated machine constants, in ohms, are $X_{aq} = 0.80$, $x_{ad} = 1.48$, and leakage reactance, $x_l = 0.165$. The no-load saturation curve is shown in Fig. 7.

Constant Load Voltage

The generator was connected with a rectifier in each of the three phases, as indicated in Fig. 1(a). To maintain substantially constant load voltage a 2600-μF condenser was connected across the load resistor. Measurements taken during testing showed that the load voltage had less than 3 percent harmonic content. Load resistance and generator dc field current were varied to obtain wide ranges of load dc voltage and current. Recorded were load dc volts, load dc current, dc field current, and load ripple voltage. The rectifier forward voltage drop was approximately 2 volts dc. Table I lists data for several tests together with calculated field current.

Calculations were carried out using the equivalent X simply equal to the calculated leakage reactance x_l. In detail, for the conditions $E_c = 80$, $I_r = 40$, $E = 2.0$, and $X = x_l = 0.165$ (ohms) we get, from (6)

$$g(u) = \frac{2\pi X I_r}{3(E_c + E)} = \frac{2\pi 0.165 \times 40}{3(80 + 2)} = 0.169.$$

Using Fig. 3, we read, for $g(u) = 0.169$, $u = 0.965$. From (2) $E_{\max} = (E_c + E)/\sin u = 82/\sin 0.965 = 100$. Fig. 5 shows that for $u = 0.965$, $H = 0.13$ and $\theta = -28°$. Using (12)

$$I_1 = H\frac{E_{\max}}{(\pi \times \sqrt{2})} = 0.13\frac{100}{\pi 0.165\sqrt{2}} = 17.7.$$

TABLE II

TEST DATA FOR CONSTANT CURRENT

Load Voltage, E_d (volts)	Load Current, I (amperes)	Field Current	
		Measured (amperes)	Calculated (amperes)
72	40	24	24
78	80	31.5	30.5
97	100	45	40

The phasor diagram, constructed as shown in Fig. 4, shows that $E_I = 89$. From the saturation curve of Fig. 7 the corresponding field current is 28 amperes, which compares well with the measured value of 29.5. For the other two test points, using the same parameters, the agreement between test and calculated field current is also good.

Constant Load Current

The machine was connected as illustrated in Fig. 1(b). Nearly constant current was maintained by connecting a spare rotor field winding in series with the load resistor. Less than 3 percent harmonic content developed across the load. As for the previous tests, load resistance and generator dc field current were varied over a wide range. Table II lists data for several of these tests.

For the $I = 100$ amperes load point we have, according to (22)

$$E_{\max} = \frac{2\pi}{3\sqrt{3}}(E_d + E) + \frac{IX}{\sqrt{3}}$$

$$\sqrt{3}\,E_{\max} = 2.09 \times (97 + 2) + 100 \times 0.165$$

$$= 207 + 16.5 = 223.5$$

or $E_{\max} = 129$. From (15)

$$\cos u = 1 - \frac{IX}{E_{\max}\sin \pi/3} = 1 - \frac{16.5}{111.7} = 0.852$$

giving $u = 0.55$.

Using Fig. 6, we find, for $u = 0.55$, $I_{\max}/I = 0.54$ and $\alpha = 82$ degrees.

Completing the phasor diagram ($\theta = \alpha - 60$, in degrees) we find that $E_I = 122$, and entering Fig. 7, the field current is read as 40. Good agreement is also obtained at the other two test points.

Discussion and Conclusions

The good agreement between test and calculated field currents, over a wide operating range, both for constant load current and constant load voltage conditions confirms the accuracy of the proposed method. In addition the method has the advantage of simplicity. Based upon data from tests on one machine only, it appears that the calculated leakage reactance may be appropriate for the equivalent reactance X.

Applications would include design and analysis studies of excitation systems for large synchronous machines, dc transmission, aerospace vehicle power supplies, and industrial rectification.

The method can be extended to other rectifier connections, including generator resistance, and also various other conduction modes. Further work should include an examination of the effect of time and space harmonics, leading to a more precise representation of the machine; tests on machines of different design and rating should also be performed.

Acknowledgment

The interest, encouragement, and support of the General Electric Company are gratefully acknowledged and appreciated.

References

[1] E. Kubler, "Rectifier load on generators and three-phase a-c systems in vector representation," *Wiss. Veroffentl.*, vol. 18, pp. 50–59, 1939.
[2] A. Schmidt, Jr. and W. P. Smith, "Operation of large dc motors from controlled rectifiers," *AIEE Trans.*, vol. 67, pp. 679–683, 1948.
[3] W. J. Shilling, "Exciter armature reaction and excitation requirements in a brushless rotating-rectifier aircraft alternator," *AIEE Trans. (Appl. Ind.)*, vol. 79, pp. 394–402, November 1960.
[4] K. G. Black, "The effect of rectifier discontinuous current on motor performance," *IEEE Trans. (Appl. Ind.)*, vol. 83, pp. 377–382, November 1964.
[5] B. Gerstmann, "Current waveshapes in rectifier circuits," *J. Eng. Educ.*, vol. 1, pp. 573–583, 1964.
[6] J. Stepina, "Calculation of the rms value of the ampere-turns per unit of rotor periphery in the synchronous machine under rectifier load," *Acta Tech. CSAV*, no. 3, pp. 255–280, 1964.

Discussion

D. I. Gorden (Westinghouse Electric Corporation, East Pittsburgh, Pa.): The paper provides a method for calculating the required dc field current of a three-phase synchronous ac generator for known dc load conditions and machine characteristics. It is felt that further work should be done leading to more precise representation of the machine as was suggested by the author. The measured field current of the generator versus the calculated field current in Tables I and II varied by 12 percent. The method did not include the following items, which directly affect the regulation: 1) resistance and inductance of the legs of the rectifier circuit; 2) rectifier modes of operation [7].

The method used the leakage reactance X_l to represent the commutating reactance. During commutation the generator sustains a line-to-line short circuit. The generator reactance that controls the short-circuit current should be used as commutating reactance. The magnitude of the X_d'' and X_q'' greatly affects both the magnitude of short-circuit current values and the commutating angle.

Once the rms generator voltage and current values are known based on regulation curve of the circuit (Ed/Ed_0 versus $IdXc/E_s$) the phasor diagram for the synchronous machine can be drawn using the author's method.

In conclusion it is important that further work should be done to include the examination and tests on machines of different design and rating. The 30-kVA three-phase 400-Hz aircraft-type generator was the testing source used to check this method. This type of unit may be satisfactory for space vehicle power applications, but it is felt that more precise representation be obtained when working with generators 10 to 300 times this rating.

References

[7] R. L. Witzke, J. V. Kresser, and J. K. Dillard, "Influence of ac reactance on voltage regulation of 6-phase rectifier," *AIEE Trans. (Commun. Electron.)*, vol. 72, pp. 244–253, July 1953.

Manuscript received February 6, 1970.

Richard T. Smith: The author wishes to thank Mr. Gorden for his excellent discussion. It is gratifying to see that we are in complete agreement.

Manuscript received March 17, 1970.